Journal of Chromatography, 483 (1989) 263–287
Elsevier Science Publishers B.V., Amsterdam — Printed in The Netherlands

CHROM. 21 937

DETERMINATION OF ION-EXCHANGE EQUILIBRIUM PARAMETERS OF AMINO ACID AND PROTEIN SYSTEMS BY AN IMPULSE RESPONSE TECHNIQUE

ROGER D. WHITLEY, JULIE M. BROWN, NANDU P. KARAJGIKAR and NIEN-HWA LINDA WANG*

School of Chemical Engineering, Purdue University, West Lafayette, IN 47907 (U.S.A.)

(First received June 14th, 1989; revised manuscript received August 29th, 1989)

SUMMARY

The application of an impulse technique to determine the Langmuir isotherm parameters of amino acids and proteins in ion-exchange chromatography is described. The ion-exchange column is approximated as many stages in series. Within each stage, the mass transfer rate of a given solute between mobile and stationary phases is finite. Responses to pulse and step changes are calculated using a fast and stable algorithm. The equilibrium parameters are estimated by comparing the responses with the experimental data. The sensitivity of the response with respect to equilibrium and mass transfer parameters was studied. The accuracy of estimation of the equilibrium parameters depends strongly on the pulse volume and pulse concentration. A methodology for selecting the proper pulse parameters was developed and successfully used to determine the equilibrium parameters of phenylalanine and bovine serum albumin.

The stage model represents pulse data as closely as a more detailed rate equation model while requiring two orders of magnitude less computation time. This technique offers a fast alternative to the conventional batch equilibrium and frontal analysis methods for determining equilibrium isotherms. The impulse technique requires fewer laboratory manipulations than the batch method and, as a result, the data are less scattered. More important, it requires only 1% as much substrate as batch methods and is of value in estimating the equilibrium parameters of costly biochemicals.

INTRODUCTION

Because of their high processing speed, mild processing conditions and good resolution characteristics, ion-exchange processes are often used in the laboratory- and preparative-scale purification of proteins and amino acids[1]. Design procedures for packed-bed ion-exchange columns are well established for linear-isotherm, single-component systems[2]. Increasingly, large feed pulses and higher solute concentrations are being used in large-scale ion-exchange processes to improve throughputs. These systems are more difficult to analyse and design because of the competition of solutes for sorbent sites. As a result, obtaining accurate estimates of non-linear equilibrium parameters for these design procedures becomes critical.

0021-9673/89/$03.50 © 1989 Elsevier Science Publishers B.V.

The conventional techniques for determining equilibrium isotherms include batch equilibrium and frontal analysis methods. In the batch equilibrium method, a known amount of resin is equilibrated with substrate solution and the adsorbed phase concentration is determined from the initial and final solution phase concentrations[3–5]. In the frontal analysis method, equilibrium parameters are calculated from the positions of the breakthrough curves[6–10]. Each of these approaches requires data from a series of individual experiments for the determination of a complete isotherm and, as a result, consumes relatively large amounts of substrates. When substrate costs or sorbent costs are high, these methods are not economical. Also, these methods require extensive manual manipulation and are very time consuming.

When the equilibrium isotherm is linear, the dynamic impulse response technique has been widely used for determining both transport and equilibrium parameters[11–15]. The parameters are estimated by matching the experimental response with the response predicted by a model that describes the transport and equilibrium relationships of the solute in the column. On the bases of cost and time, this technique offers considerable advantages over the batch methods. In terms of equipment, the use of microbore columns would reduce the amounts of substrates required even further, and the current technique is also applicable to those systems.

Some groups have extended the impulse response technique to estimate non-linear equilibrium parameters[16,17]. They showed that with a reasonably good transport model (which accounts for band speading due to mass transfer resistance), the non-linear equilibrium parameters can be estimated accurately. Kirkby *et al.*[16] successfully used this technique to determine the equilibrium parameters of Freundlich isotherms in reversed-phase chromatography.

This paper reports the use of an impulse response technique with a stage model to determine isotherm parameters of proteins and amino acids for ion-exchange chromatography. In general, the model may be used with any desired isotherm. For the systems studied, the Langmuir isotherm is used. The key areas of interest are the sensitivity of the model to the parameters, pulse size and concentration necessary to estimate the parameters accurately, and verification of the parameter estimates by the batch method. The model is also compared with a much more complex rate model developed previously by Yu and Wang[18] which considers axial dispersion, film and intraparticle diffusional resistances in addition to non-linear isotherms. The corresponding set of equations requires a great deal of computation to simulate a pulse response. For the same pulse experiments, the two methods simulate the response equally well, and the stage model requires two orders of magnitude less calculation time.

THEORY

As illustrated in Fig. 1, the stage model approximates the axial dimension of the column as a series of N equal volume (V) stages. The mobile phase flows through these well mixed stages at a rate Q. Within each stage the total volume is divided into three fractions: the bulk solution ($V\varepsilon_b$), the pore solution $[V(1 - \varepsilon_b)\varepsilon_p]$ and the solid phase $[V(1 - \varepsilon_b)(1 - \varepsilon_p)]$, where ε_b is the bed void fraction and ε_p is the intraparticle void fraction. For a given stage, a concentration gradient exists between the bulk solute concentration, P, and the pore solute concentration, P^*. This concentration difference

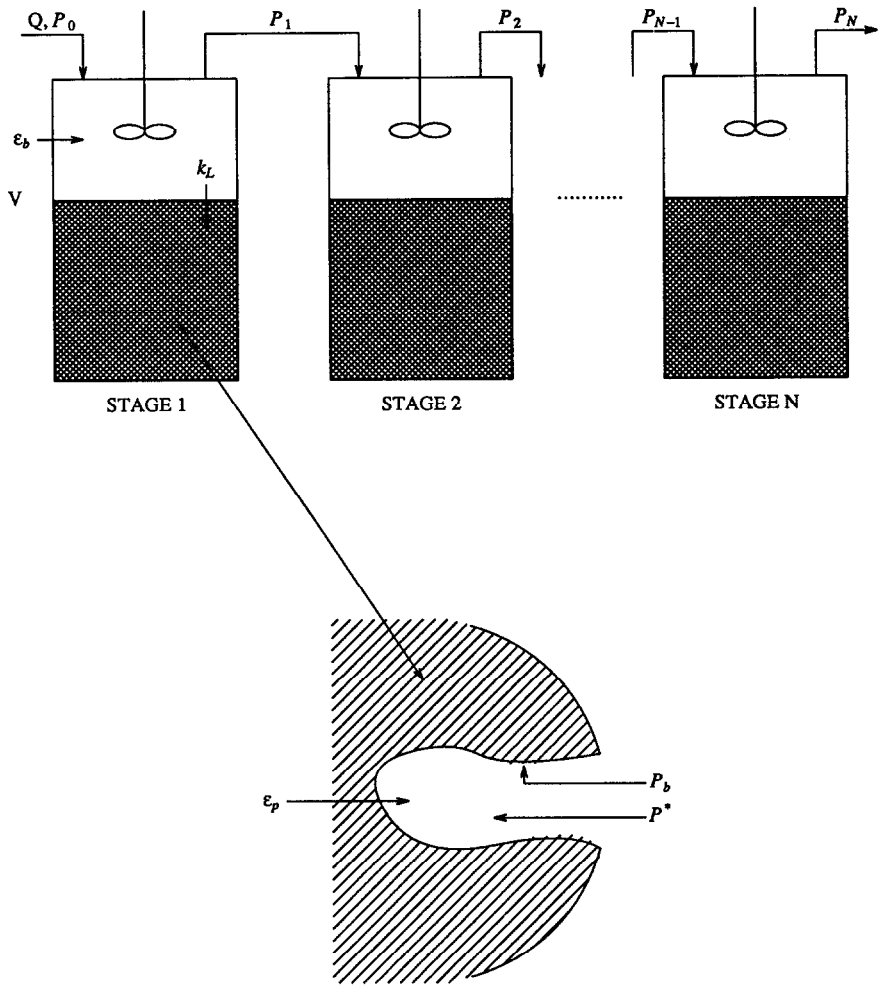

Fig. 1. Schematic diagram of the stage model approach for this system.

results from the combined effects of the film and pore diffusion mass transfer resistances. The solute concentration in the pores is taken as an average value.

Equilibrium, assumed between the solute in the pore solution and the solute on the solid phase, P_b, is described by a two-parameter Langmuir equation. The ion-exchange process between P and a monovalent species C can be described as

$$P^{\pm Z} + ZC_b \rightleftharpoons P_b + ZC \tag{1}$$

The resulting mass action equation is[5,19]

$$P_b = KP\left(\frac{P_m - P_b}{C}\right)^Z \tag{2}$$

When the binding number, Z, is unity, eqn. 2 may be simplified to

$$P_b = \frac{KP_m P}{C + KP} \tag{3}$$

As the total ion concentration in the bulk phase is a constant, we can define $C_T \equiv C + P$ and eliminate C from eqn. 3:

$$P_b = \frac{\left(\frac{KP_m}{C_T}\right) P}{1 + \left(\frac{K-1}{C_T}\right) P} = \frac{aP}{1 + bP} \tag{4}$$

and only one parameter, K, determines the isotherm. If the value of Z is not unity, Whitley *et al.*[5] have shown that the two-parameter Langmuir equation (a and b fitted independently) still represents the ion-exchange equilibria of proteins well. For these reasons, the Langmuir equation is used in this paper.

Band spreading of a pulse is due to a combination of axial dispersion, film mass transfer and pore diffusion. Axial dispersion results from path tortuosity and from wall effects (flow becomes slow very close to the particle surface). The effects of axial dispersion are well described by adjusting the number of stages used in this model. Transport of solute from the bulk mobile phase to the resin surface and subsequent diffusion in the pores can be represented by film mass transfer and pore diffusion terms. If the concentration profile in the resin pellet is parabolic, then the two phenomena may be represented by a simple linear driving force[20] consisting of the difference between the bulk and pore concentrations, $P - P^*$, weighted by an overall mass transfer coefficient.

Based on the above assumptions, the following mass balance equations are derived. For stage 1, mobile phase and resin phase mass balances give

$$Q P_0 - Q P_1 - \frac{3}{R}(1 - \varepsilon_b) V k_L [P_1 - P_1^*] = \varepsilon_b V \cdot \frac{dP_1}{dt} \tag{5}$$

$$\frac{3}{R}(1 - \varepsilon_b) V k_L [P_1 - P_1^*] = (1 - \varepsilon_b)\varepsilon_p V \cdot \frac{dP_1^*}{dt} + V \cdot \frac{dP_{1,b}}{dt} \tag{6}$$

Substituting

$$\theta = t/\tau \tag{7a}$$

$$\tau = NV\varepsilon_b/Q \tag{7b}$$

and

$$\frac{dP_{1,b}}{dt} = \frac{dP_{1,b}}{dP_1^*} \cdot \frac{dP_1^*}{dt} = f'(P_1^*) \cdot \frac{dP_1^*}{dt} \tag{7c}$$

into eqns. 5 and 6, one obtains

$$\frac{dP_1}{d\theta} = N(P_0 - P_1) - \frac{3\tau k_L}{R} \cdot \frac{(1-\varepsilon_b)}{\varepsilon_b}(P_1 - P_1^*) \tag{8}$$

$$\frac{dP_1^*}{d\theta} = \frac{3k_L\tau}{R}(P_1 - P_1^*)\Big/\left[\varepsilon_p + \frac{f'(P_1^*)}{(1-\varepsilon_b)}\right] \tag{9}$$

where $f'(P_1^*)$ is the derivative of the Langmuir expression (eqn. 4):

$$f' = \frac{a}{(1+bP^*)^2} \tag{10}$$

For stages $2 \leqslant j \leqslant N$, the mass balance equations may be written similarly as

$$\frac{dP_j}{d\theta} = N(P_{j-1} - P_j) - \frac{3\tau k_L}{R}\left(\frac{1-\varepsilon_b}{\varepsilon_b}\right)(P_j - P_j^*) \tag{11}$$

$$\frac{dP_j^*}{d\theta} = \frac{3\tau k_L}{R}(P_j - P_j^*)\Big/\left[\varepsilon_p + \frac{f'(P_j^*)}{(1-\varepsilon_b)}\right] \tag{12}$$

As can be seen, approximating the column as a series of discrete stages reduces the resulting equations to a set of ordinary differential equations rather than a set of partial differential equations.

For a rectangular pulse input of duration 0 to θ_p, the initial and boundary conditions are

$$P_0 = \begin{cases} P_P & 0 \leqslant \theta \leqslant \theta_P \\ 0 & \theta > \theta_P \end{cases} \tag{13}$$

Subject to the initial and boundary conditions given by eqn. 13, eqns. 8, 9, 11 and 12 are solved numerically by "A Differential/Algebraic System Solver" (DASSL) to determine the response[21]. Calculations are performed with double precision, and all numerical tolerances are set to insure four significant digits in the time and concentration values of the model curve. Hence the numerical contribution to dispersion is negligible. For any given set of the parameters (a, b and k_L), the model predicts a unique effluent history. This prediction may be compared with the actual effluent history. The parameter values of a, b and k_L can be estimated by minimizing the error between the experimental and the model response curves. The parameter search is conducted by the IMSL (International Mathematical and Statistical Libraries, Edition 10, Houston, TX, U.S.A.) routine DUNLSF, which employs a finite difference Levenberg–Marquardt algorithm with strict descent. The criterion for minimization is defined as

$$\Phi_A = \frac{1}{m}\Sigma(P_{exp} - P_{model})^2 \tag{14a}$$

where m is the number of points used from the effluent history curve. A fit based on absolute error works better, as a relative error fit gives too much emphasis to the tail of the pulse. Some of the tailing may be caused by extra-column effects and slow kinetics at the surface. These effects are not explicitly considered in the model; however, they are effectively lumped into k_L. In order to compare the fit among different experiments, a relative error, Φ_R is also calculated:

$$\Phi_R = \frac{1}{m} \Sigma \left(\frac{P_{exp} - P_{model}}{P_{exp}} \right)^2 \tag{14b}$$

Between 40 and 110 experimental data points (m) were used in the optimization process. Calculated P_{model} values were compared with P_{exp} and used in the computation of Φ_A and Φ_R.

Non-linear isotherms were studied by moment analysis for the limiting case of a single slurry tank[22]. In Dogu's work[22], the technique uses the second moment and is limited to small deviations from linearity in a Langmuir isotherm. The second moment is really a variance and, as such, is only additive when linearly dependent on the sources of variance. Stage models are not limited in this way if mass transfer is accounted for.

The well known Thomas solution to the ion-exchange problem[23] uses a Langmuir expression with only one empirically determined parameter (derived from monovalent exchange kinetics with the assumption that the total capacity of the column is known). The stage model of this work uses a two-parameter Langmuir expression. The Thomas model driving force is based on the difference of the bulk solute concentration from its equilibrium value with respect to the solid-phase concentration. In the current study, the driving force is the difference between the bulk solute concentration and an averaged pore concentration. This approach has the advantage of considering the pore concentration, where as the Thomas model ignores it.

EXPERIMENTAL

The two systems investigated were phenylalanine (PHE) on AG 50W (Bio-Rad Labs.) and bovine serum albumin (BSA) on DEAE-Sepharose Fast Flow (Pharmacia). In the PHE–AG 50W system, sodium citrate buffer was used to maintain the pH. The

TABLE I

PHYSICAL AND CHEMICAL PROPERTIES OF THE SORBENTS

Parameter	*DEAE-Sepharose*	*AG 50W-X8*
Functional group	Diethylaminoethyl	Sulfonic acid
Type	Gel	Gel
Exchange capacity (equiv./ml)	$8.4 \cdot 10^{-5}$	$1.7 \cdot 10^{-3}$
Particle diameter (μm)	45–165	65–135
Intraparticle void fraction	0.95	0.52
Bead structure	6% cross-linked	8% cross-linked
Manufacturer	Pharmacia	Bio-Rad Labs.

total concentration was 0.16 or 0.2 *M* and the data were obtained at pH 2.0, 3.0 and 4.0. In the BSA–DEAE Sepharose system, Tris–HCl buffer (0.10 *M*) was used to maintain the pH at 8.0. The chloride concentration was controlled by addition of sodium chloride before the pH was adjusted. Data were collected at Cl^- concentrations of 0.13 and 0.16 *M*. The physical and chemical properties of the sorbents are summarized in Table I.

Batch equilibrium experiments

Values of the equilibrium constant for the PHE–AG 50W system, determined by the batch equilibrium method were taken from the paper by Wang *et al.*[24]. BSA equilibrium isotherms were obtained at pH 8.0 for 0.13 and 0.16 *M* Cl^- concentrations. Protein solutions were prepared by dissolving known amounts for the protein in the appropriate buffer solution at a concentration of 0.2–35 mg/ml. Aliquots of 3 ml of solution were equilibrated with about 1.0 ml of ion-exchanger suspension (*ca.* 50 vol.-%) on a rotating shaft for 24 h. The protein concentration in the equilibrium samples was determined by measuring the UV absorbance at 280 nm with a Perkin-Elmer Lambda 3A spectrophotometer. Equilibrium isotherms were obtained from the initial and equilibrium concentrations by applying mass balance principles[25].

Pulse response experiments

Buffer solution was pumped by a WIZ peristaltic pump from a reservoir to a Rheodyne Type 50 rotary valve. A variable-volume loop was used to inject protein pulses of desired concentrations into the column. The column was a 1.0 cm I.D. glass column packed to the desired height. The column was presaturated with the buffer solution to be used in the isocratic elution experiment. The procedure for packing and equilibrating the column was reported by Brown[25]. The column outlet was connected to a Helma quartz flow cell. The absorbance of the column effluent was monitored at 280 nm and recorded by a Perkin-Elmer R100A recorder. Pulse input was used to determine the isotherm parameters of BSA on DEAE-Sepharose. The PHE–AG 50W system was investigated by measuring the elution curve of a presaturated column. PHE effluent was monitored at 254 nm.

The dead volume was kept to a minimum. Measuring the first moment of the response through only the tubing gave the dead volume. The total colum void fraction was measured similarly by injecting a small non-adsorbing species (nitrate on the

TABLE II

ELUTION EXPERIMENTAL CONDITIONS (PHE–AG 50W)

Run	*pH*	*L* (*cm*)	*Q* (*ml/min*)	P_0 (*M*)	C_T (*M*)
1	2.0	7.2	1.0	0.017	0.16
2	3.0	8.0	0.95	0.02	0.2
3	3.0	6.8	1.0	0.1	0.2
4	4.0	10.5	1.1	0.018	0.2
5	4.0	6.5	1.0	0.02	0.2
6	4.0	6.8	1.0	0.1	0.2

TABLE III

PULSE EXPERIMENTAL CONDITIONS (BSA–DEAE-SEPHAROSE, pH 8.0)

Run	C_0 *(M)*	L *(cm)*	Q *(ml/min)*	V_P *(ml)*	P_P *(mg/cm³)*
1	0.13	4.0	2.5	0.10	10
2	0.13	4.0	2.5	0.25	10
3	0.13	4.0	2.5	0.50	10
4	0.13	4.0	2.5	1.00	10
5	0.13	4.0	2.5	2.01	10
6	0.13	4.0	2.5	2.95	10
7	0.13	4.0	2.5	5.00	10
8	0.13	4.0	2.5	2.01	20.1
9	0.13	4.0	2.5	2.95	20.1
10	0.16	3.2	0.50	0.10	20
11	0.16	3.2	0.75	0.10	20
12	0.16	3.2	1.00	0.10	20
13	0.16	3.2	1.00	0.25	20
14	0.16	3.2	2.35	5.00	1.0
15	0.16	3.2	2.35	2.01	14
16	0.16	3.2	2.11	0.10	10
17	0.16	3.2	2.11	0.25	10
18	0.16	3.2	2.11	0.50	10
19	0.16	3.2	2.11	1.00	10
20	0.16	3.2	2.58	2.95	10

cation exchanger CM-Sepharose) into the column. The interparticle void fraction was measured by injecting a large non-adsorbing species which was excluded from the pores. The intraparticle void fraction was then calculated from the total void fraction and the interparticle void fraction[25]. The elution and pulse experimental conditions are given in Tables II and III, respectively.

RESULTS AND DISCUSSION

Sensitivity analysis of the response

As the parameters are estimated from the measured response, it is important to know the relationship between each parameter and the position or shape of the response curve. In order to perform this analysis, a series of simulations were conducted using the following system parameters: column length, $L = 3.5$ cm; bulk flow-rate, $Q = 2.5$ ml/min; pulse volume, $V_P = 1.00$ ml; and pulse concentration, $P_P = 10.0$ mg/ml. These values apply to Figs. 2–8 and 10. For a given set of parameters, the stage model program calculates P, P^* and P_b in each stage of the column. Representative values of these variables for the last stage during a pulse experiment are shown in Fig. 2.

For continuous-flow systems, such as the ion-exchange system under study, approximating the spatial direction as a series of stages allows one to model axial dispersion by altering the value of N. As shown in Fig. 3a decreasing values of N imply increasing axial dispersion (increased band spreading and asymmetry). It is clear that this effect is axial dispersion as it can occur even for linear isotherms ($b = 0$) and

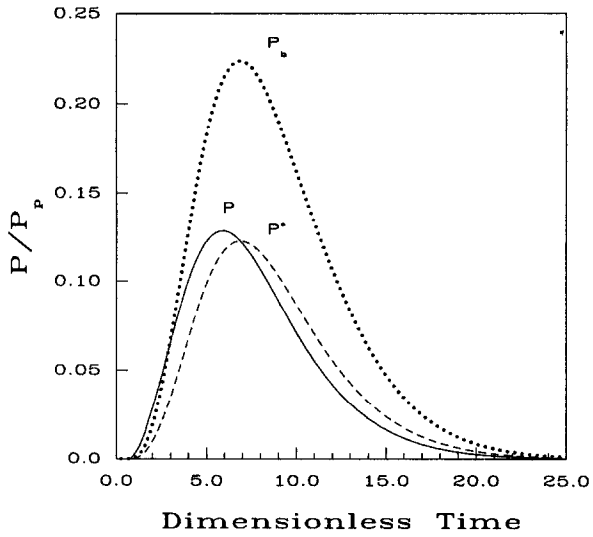

Fig. 2. Relative values of bulk solution, pore and bound protein concentrations in the last stage (a = 2.0, b = 0.08 ml/mg, k_L = 0.015 cm/min).

negligible mass transfer resistance (k_L = 100.0, 3.5 orders of magnitude greater than observed for the BSA system; see Fig. 3b).

For this system at Q = 0.84 ml/min, Yu and Wang[18] obtained an axial Peclet number of Pe_b = 393. Wankat[26] gave the relationship $2N = Pe_b$ for linear systems and negligible mass transfer resistance. Even though the system under study is far from linear, the relationship still may serve as a first-order approximation for N. Using this relationship, we obtained N = 196. Considering Fig. 3a, it can be seen that $N > 75$ has no significant effect on the curve shape or position for the average values of a and b in this system. As axial dispersion does not contribute noticeably to band spreading, N is set equal to a high value (100). If band spreading due to mass transfer is reduced (by increasing k_L), the band spreading due to axial dispersion becomes more noticeable. This effect may be seen by noting the increased difference betweeen curves for 75 and 100 stages on going from Fig. 3a to 3b. If there are extra-column contributions to band spreading (such as long tubing paths or poor connections), these will appear in the k_L term.

Fig. 4 shows the effect of k_L. As the axial dispersion effects are negligible, the only factor governing the peak broadening is the overall mass transfer coefficient, k_L. One may be tempted to conclude that the asymmetry in Fig. 4 is due to the non-linear isotherm. However, the same curves generated with b = 0 are still asymmetric. This indicates that slow mass transfer rates can also cause asymmetry. If mass transfer into the paticle is very slow (small k_L), part of the solute pulse goes directly through the column without being adsorbed, and this can result in band splitting as shown in Fig. 4. This effect has been noted in other studies of mass transfer effects on pulse experiments[17,27].

Estimation of non-linear model parameters is usually complicated by insensitivity of the model to a parameter's value for a give set of experimental conditions or by

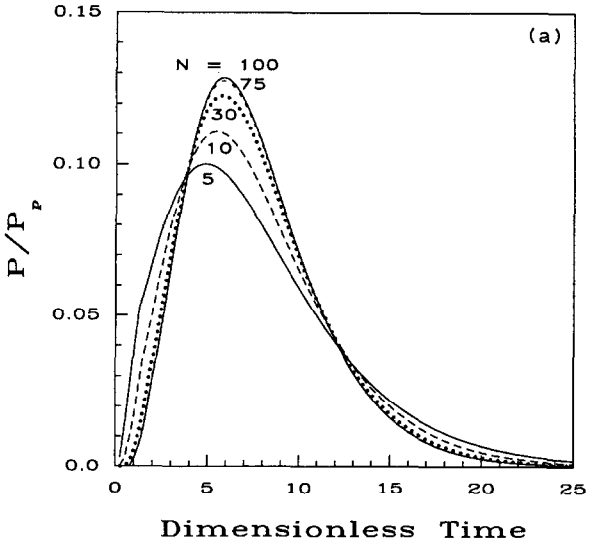

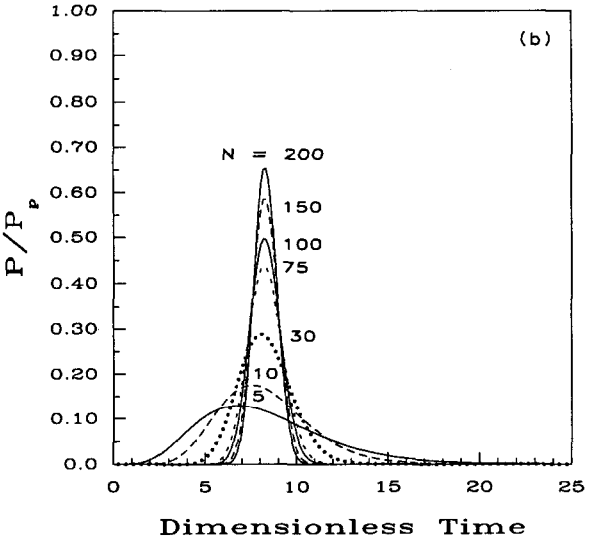

Fig. 3. (a) Effect of parameter N on the response. The fixed parameters are $a = 2.0$, $b = 0.08$ ml/mg, $k_L = 0.015$ cm/min. (b) Band spreading caused by dispersion alone. The fixed parameters are $a = 2.0$, $b = 0$ ml/mg, $k_L = 100.0$ cm/min.

correlation among the various parameters. Correlation indicates that the value of one parameter affects the value of other parameters when one is trying to minimize error during fitting. Thus, correlation is a measure of the interdependence between two parameters. To study sensitivity and correlation, a model curve was obtained using the stated values of a, b and k_L. Then model curves were generated for pairs of perturbed

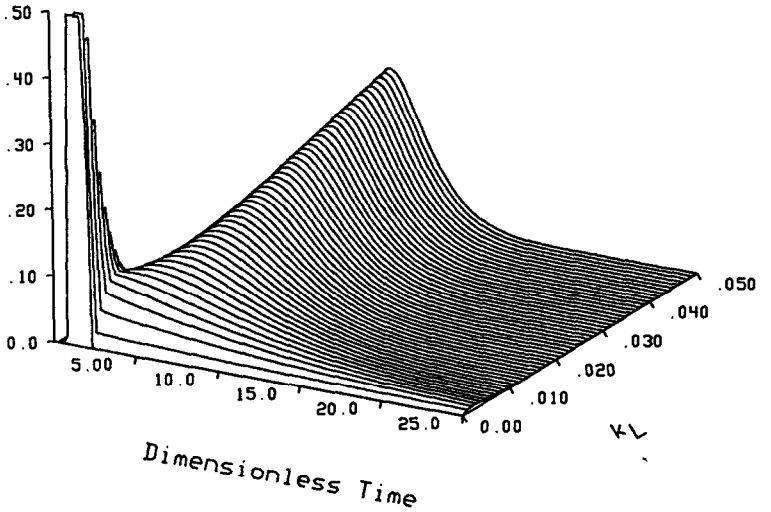

Fig. 4. Effect of k_L (cm/min) on the response. The fixed parameters are $a = 2.0$, $b = 0.08$ ml/mg, $N_A = 100$. The tops of the sharp peaks extend almost to $P/P_F = 1.00$; they have been cut at 0.5 for clarity.

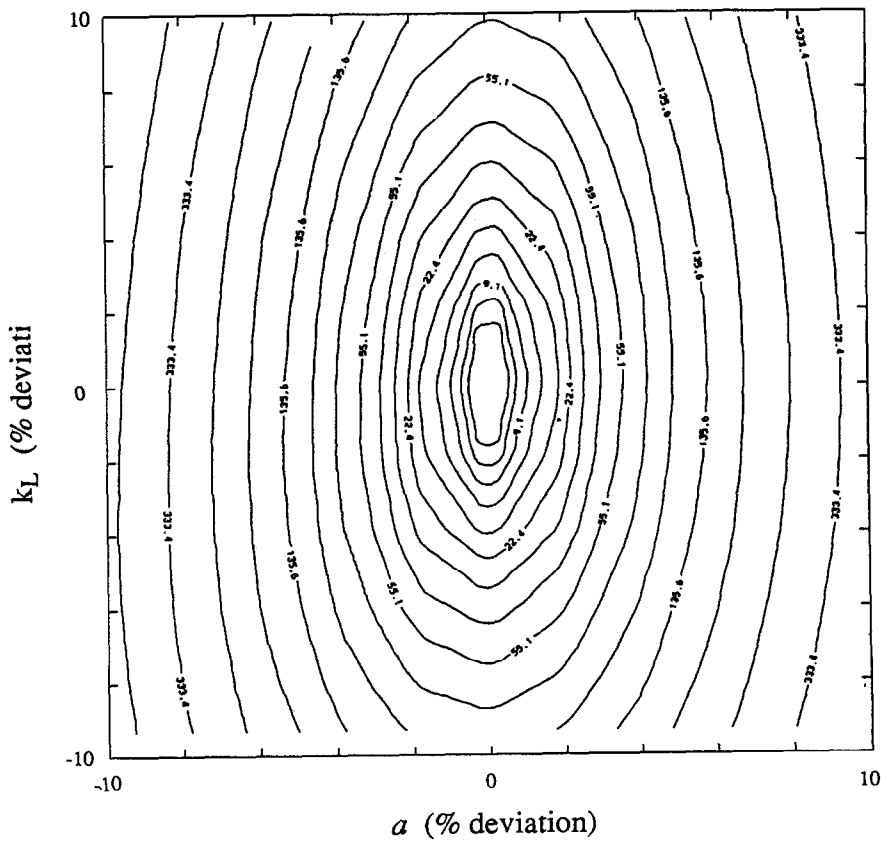

Fig. 5. Contours of k_L (cm/min) *vs.* a. The reference parameter values are $a = 2.0$, $b = 0.08$ ml/mg, $k_L = 0.015$ cm/min, $N = 100$.

values of the two parameters being varied. Corresponding sum of squares of error (*SSE*) values were obtained by comparison with the orginal curve:

$$SSE = \sum_{i=1}^{m} (P - \hat{P})^2 \tag{15}$$

A contouring package, given this grid of *SSE* values, produced a graph of constant *SSE* curves which are known as contours.

Figs. 5 and 6 show the sensitivity of the model to various combinations of k_L and a and of k_L and b, respectively. In Fig. 5, there is no correlation between k_L and a as the oval is aligned with one of the axes. The error increases more steeply for changes in a, indicating that the model is more sensitive to the value of a under the given conditions. Using the same reasoning, it can be seen from Fig. 6 that k_L and b are not correlated. Hence they may be estimated independently. In this case the model is more sensitive to the value of k_L than of b.

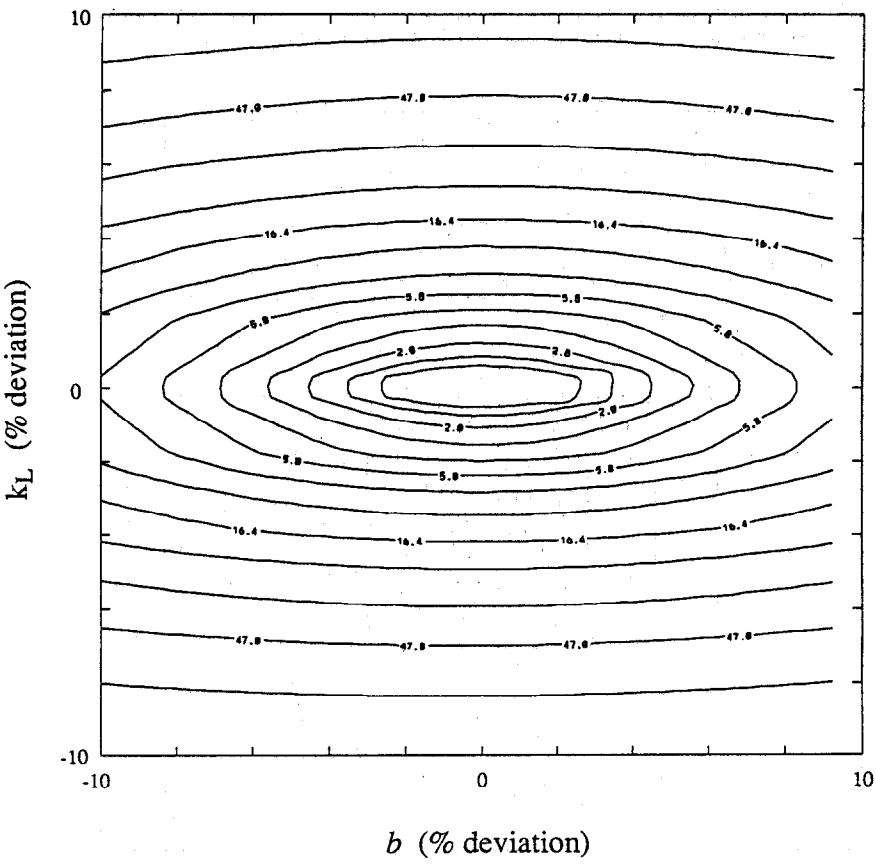

Fig. 6. Contours of k_L (cm/min) *vs.* b (ml/mg). The reference parameter values are $a = 2.0$, $b = 0.08$ ml/mg. $k_L = 0.015$ cm/min, $N = 100$.

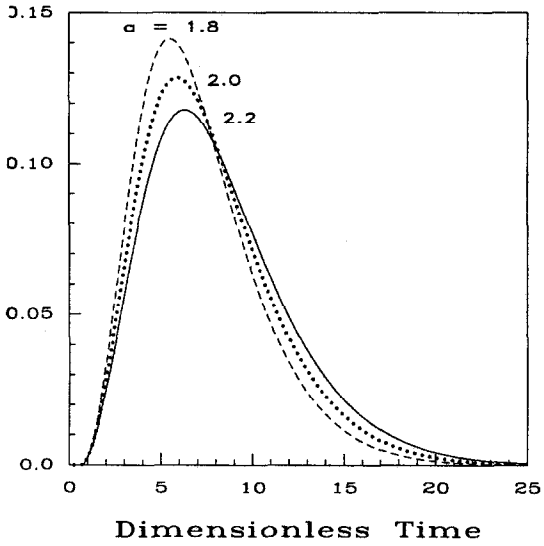

Fig. 7. Effect of a on the response. The fixed parameters are $b = 0.08$ ml/mg, $k_L = 0.015$ cm/min, $N = 100$.

Figs. 7 and 8 show the effects of the parameters a and b, respectively, on the response. As can be seen, a affects the retention time and hence the degree of band spreading. The value of b affects the height and trailing edge position of the curve. The relative importance of a and b depends on the solute concentration; b has little effect on isotherm character at low concentration and becomes more important as concentration increases. The two most direct ways to increase the average concentration in the

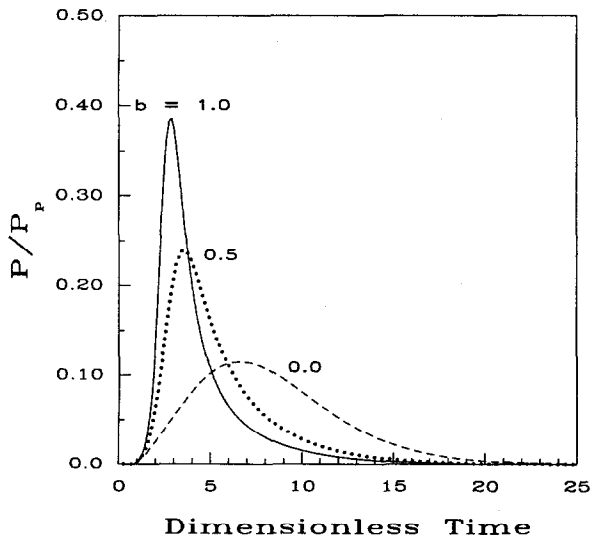

Fig. 8. Effect of b (ml/mg) on the response. The fixed parameters are $a = 2.0$, $k_L = 0.015$ cm/min, $N_A = 100$.

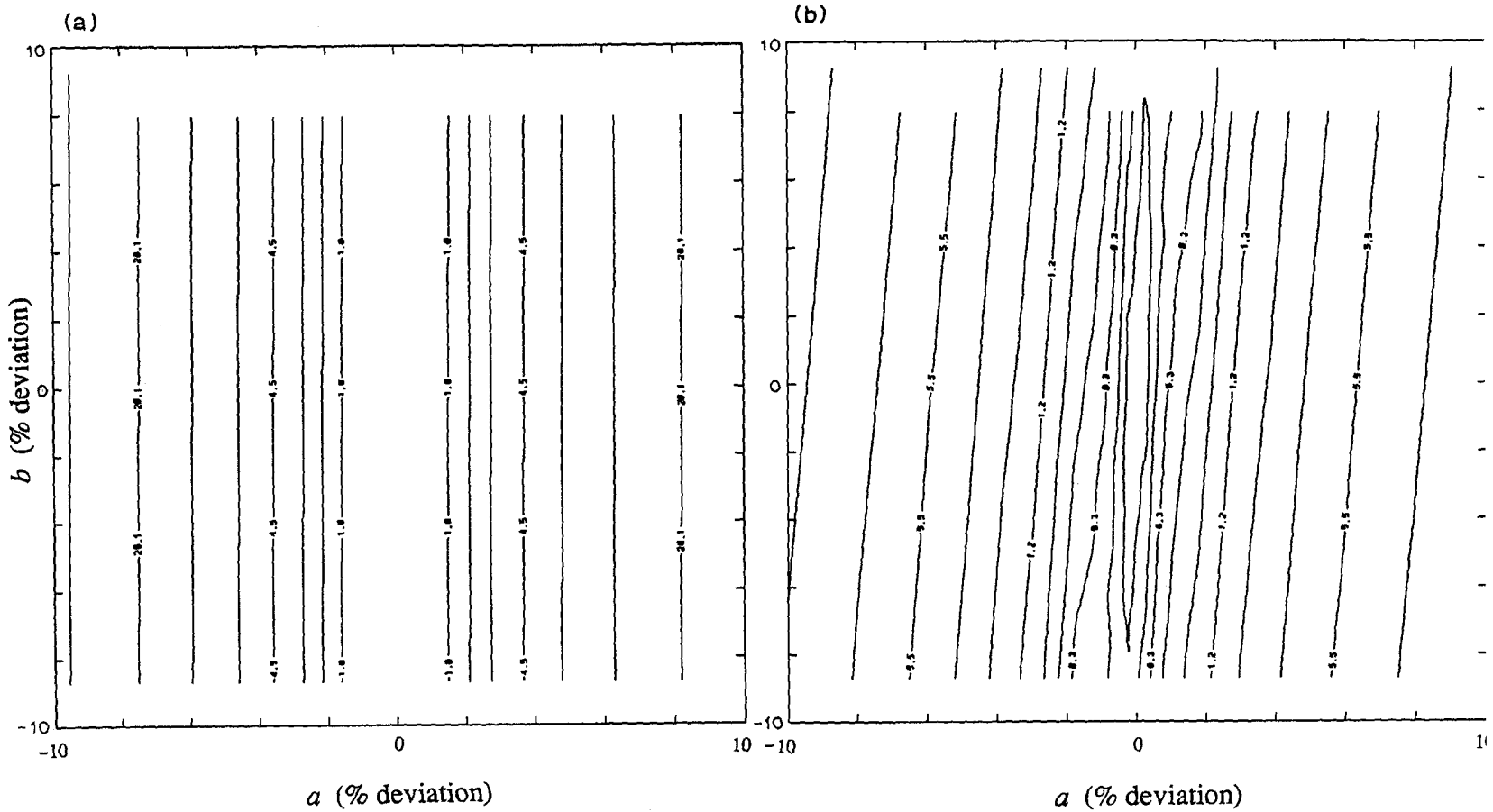
(a)
(b)
10
0
-10
b (% deviation)
a (% deviation)

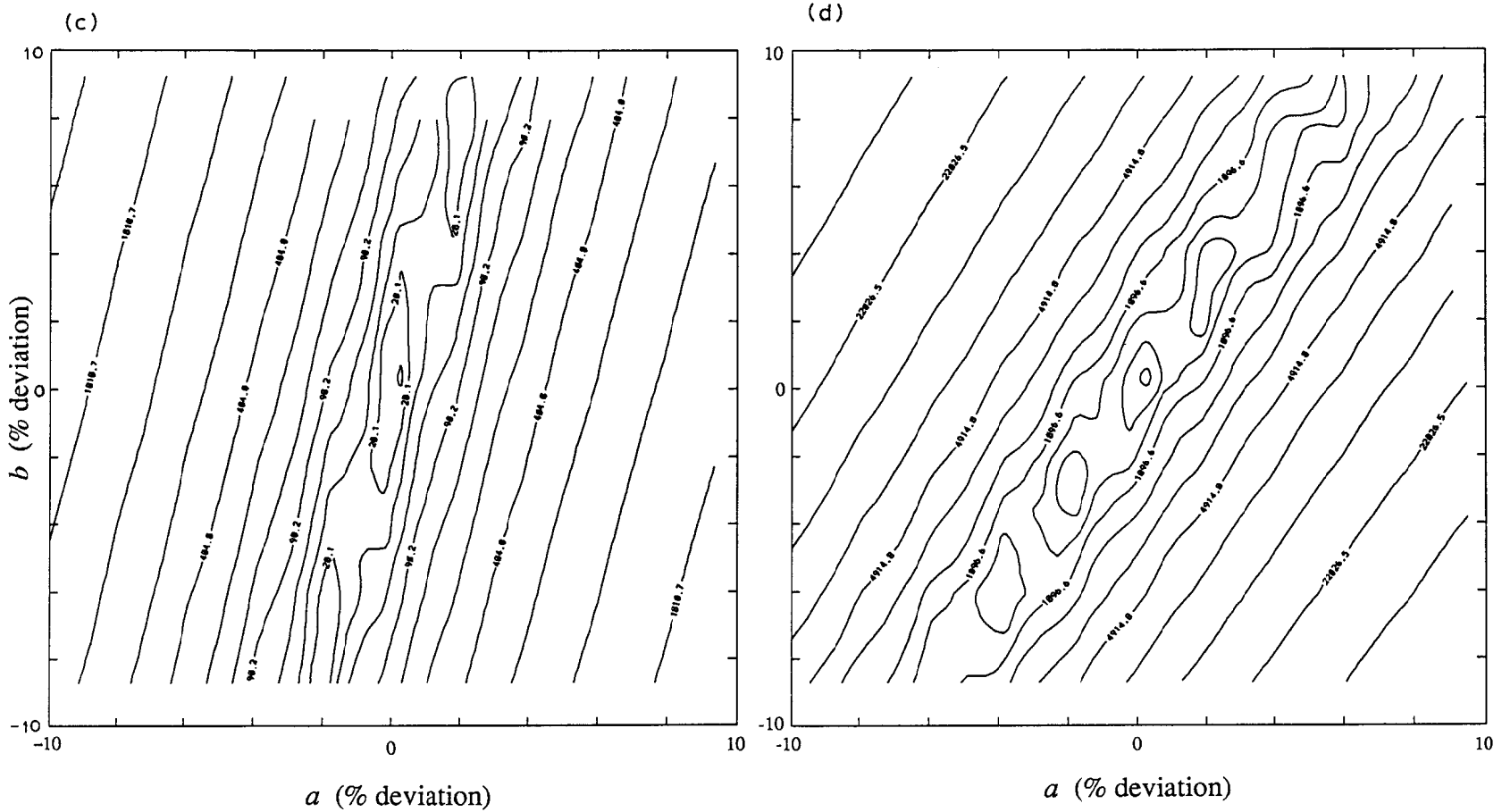

Fig. 9. Contours of b (ml/mg) *vs.* a. The reference parameter values are $a = 2.0$, $b = 0.08$ ml/mg, $k_L = 0.015$ cm/min, $N = 100$; $P_P =$ (a) 1.0, (b) 20.0, (c) 20 and (d) 20 mg/ml; $V_P =$ (a) 0.30, (b) 0.30, (c) 1.0 and (d) 5.0 ml.

system are to increase the pulse concentration, P_P, and to increase the pulse volume, V_P. In Fig. 8, for $b = 0$, the peak is asymmetric; this is due to a large mass transfer resistance, as the isotherm is linear.

Fig. 9a and b show contours of b *versus* a at pulse concentrations 1 and 20 mg/ml, respectively. At low values of P_P, the equilibrium isotherm is linear and is given by $P_b = a P$. Fig. 9a indicates that a may be well estimated at $P_P = 1$ mg/ml but not b, as the error does not increase greatly for the changes in b observed on the contour. As the pulse concentration is increased, a and b become correlated (as shown by the trough rotating off the b axis slightly). This implies that estimation of b becomes more reliable as the pulse concentration increases as b gains more effect on the *SSE*. However, in Fig. 9b, although the innermost contour does close, it is extremely elongated. By increasing the pulse volume from 0.30 to 1.0 ml (Fig. 9b *versus* Fig. 9c), the contours are greatly shortened and rotated further off the a axis, and the ability to estimate b is improved.

For even higher pulse volumes (Fig. 9d, $V_P = 5$ ml), the contours become steeper, moving away from the minimum, and clearly enclose a minimum at the center of the graph. Consequently, the minimum is more defined and the estimate of b becomes more reliable. This improvement stems from an indirect effect. Increasing the pulse volume forces the peak concentration of the pulse to increase; this in turn increases the value of P^*. Also note that the contours are now diagonal, indicating that the error depends on the ratio a/b. P^* has become so large at this point that the Langmuir isotherm (eqn. 4) simplifies to $P_b = a/b$, hence the dependence.

Fig. 10 shows the underlying reason: as the pulse volume increases, the bulk concentration (and hence the pore and adsorbed concentration) increases. The ability to estimate b accurately depends on the magnitude of P^*, which in turn depends on P_P and V_P. As P_P is usually kept as large as possible, the primary variable is V_P.

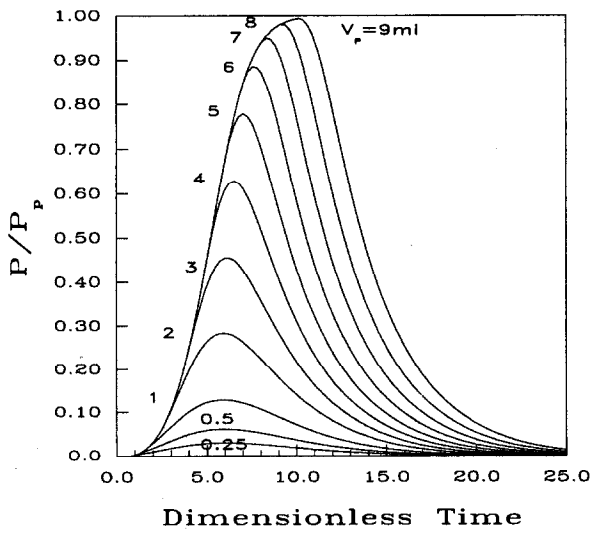

Fig. 10. Effect of increasing the pulse volume on effluent concentration; $a = 2.0$, $b = 0.08$ ml/mg, $k_L = 0.015$ cm/min.

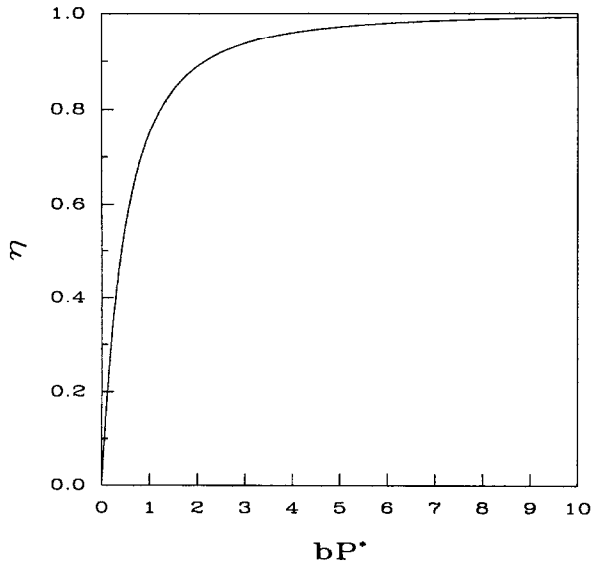

Fig. 11. Non-linearity factor η for the Langmuir isotherm.

Determination of a V_P which results in reliable estimates of b is argued in detail, and a strategy to determine b is offered below.

The combined values of V_P and P_P should be high enough to cover the non-linear range of the isotherm. Because of mass transfer effects, the actual concentration in the pores will be less than the pulse concentration. These values of V_P and P_P should compensate for the mass transfer effects. We define a non-linearity factor η as 1 minus the ratio of the slope of the isotherm at any value of P to the initial slope of the isotherm. For the Langmuir isotherm, η is given by

$$\eta = 1 - \frac{1}{(1 + bP)^2} \tag{16}$$

Fig. 11 shows the plot of η *versus* bP^*. From experience, a value of $\eta = 0.5$ implies sufficient non-linearity to estimate the value of b. This corresponds to $bP^* = 0.414$, so the minimum pore concentration sufficient to estimate tha value of b is given by

$$P^*_{\text{min}} = 0.414/b \tag{17}$$

Thus, one begins with a guessed value of b and calculates the minimum value of P^*. Noting that P^* in Fig. 2 is only a few percent less than P, let $P \approx P^*$. P_P is generally set by upstream processes or fixed at a maximum value based on solubility concerns. One can then find the minimum value of P/P_P in Fig. 10 and read off the corresponding value of V_P for a given system. Next, the experimental elution of the pulse is conducted at those conditions. The values of a, b and k_L are then fitted to the experimental data; if the values differ from the initial guesses by more than 5–10%, Fig. 10 should be regenerated for the new parameter estimates and the procedure repeated. The runs for

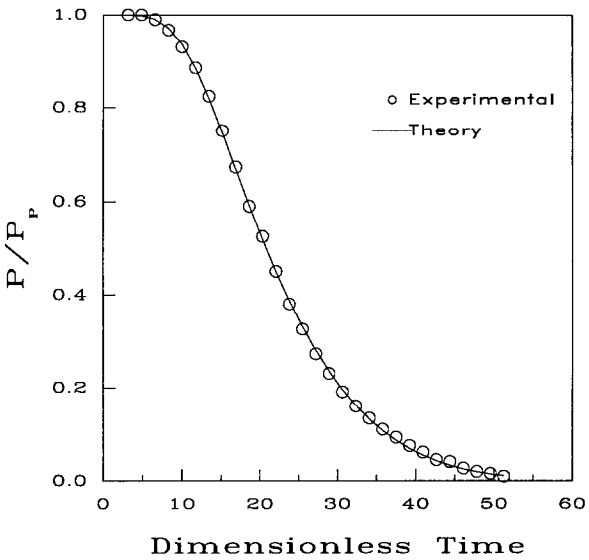

Fig. 12. Typical fit between the response determined from the model using the estimated parameter values (PHE–AG 50W, Table IV, run 2) (solid line) and the experimental response (○).

the various volumes in Fig. 10 can be generated with only 30 min of CPU time on a Gould NP1.

Experimental results

As the effective charge on the phenylalanine molecule is unity, the isotherm is determined solely by K. For BSA, the effective charge is more than 1 and, for the reason mentioned earlier, the isotherm is approximated by eqn. 4 with a and b as the isotherm parameters.

The pulse experiment is preferred as it consumes less time and material. Step elution experiments have been analyzed to demonstrate that the model can handle

TABLE IV

FITTED PARAMETERS FOR PHE–AG 50W SYSTEM

Step response							*Batch:*[a]
							K
Run	*pH*	*a*	*b (ml/mg)*	*K*	k_L *(cm/min)*	Φ_R	
1	2.0	31.49	0.225	2.96	0.022	0.0091	3.27 ± 0.27
2	3.0	12.24	0.100	1.44	0.0082	0.0029	0.60 ± 0.27
3	3.0	6.716	0.0026	0.79	0.0049	0.1805	0.60 ± 0.27
4	4.0	4.688	0.190	0.55	0.011	0.0135	0.15 ± 0.27
5	4.0	4.706	0.136	0.55	0.0085	0.1256	0.15 ± 0.27
6	4.0	2.247	−0.003	0.26	0.0038	0.0228	0.15 ± 0.27

[a] Values from ref. 24.

a variety of initial and boundary conditions. The fitting of phenylalanine elution curves was well described by this stage model, as shown by a typical model fit in Fig. 12. The parameters fitted from the experimental curves are shown in Table IV. The values of K from the elution experiments were calculated from the Langmuir a values because the b values are not as well estimated at lower concentrations. Both the step response and the batch methods agree that the PHE affinity drops sharply as the pH increases from 2.0 to 4.0. The explanation of this pH dependence has been reported elsewhere[24].

The step elution values for K do not drop as rapidly as those for the batch method. The disagreement stems from the initial solute concentration on the exchanger. The batch experiments were performed with a bulk solute concentration of about 0.1 M while the initial concentration in the column was only 0.017–0.02 M for runs 1, 2, 4 and 5 in Table IV. This apparent variation of K with PHE concentration can be explained by the presence of binding sites with different affinities. For a system with heterogeneous bindings, the lower concentration means that only high-affinity binding will be important. As a result, the average affinity will be high. When the substrate concentration increases, the average affinity will decrease as lower affinity sites also become occupied[24,28]. The difference between the step elution and batch estimates is a consequence of this concentration dependence. For runs 3 and 6 in Table IV, the step elution experiment was performed at the same initial concentrations as the batch experiments and the agreeent with the batch estimates of K improved greatly. In both instances, the estimates of K are within the experimental error of the batch estimates. This series of experiments shows that one should obtain isotherm data in the region of expected operation as the affinities may depend strongly on concentration.

Parameter values estimated from the impulse response and batch equilibrium methods for the BSA system are reported in Table V. The Φ_R values are also reported so that fits between model and data can be compared for the various experiments. The film mass transfer and the intraparticle diffusional resistances are lumped into the parameter k_L. When the superficial velocity through the column is increased, the rate of film mass transfer increases. This in turn increases the lumped mass transfer coefficient. The increase will not be noticeable, however, unless the film mass transfer resistance is significant. In Table V, runs 10–12 show that k_L does increase as the fluid flow-rate is increased (0.50–1.0 ml/min). These runs were conducted at the lower end of the range of flow-rates studied. For the runs at the higher flow-rates, k_L seems to have reached an upper limit. This indicates that the film mass transfer rate is so fast that intraparticle mass transfer resistance now dominates.

Although one might think that the bulky BSA molecules (molecular weight 67 000) would diffuse much slower than the smaller PHE molecules (molecular weight 165), the k_L values estimated for the compounds are within the same order of magnitude. This is partially because the two systems show significant film mass transfer resistance at low flow-rates. As k_L is an overall mass transfer coefficient, it depends on many factors, including film and intraparticle diffusion and the slope of the equilibrium curve[2]. In the light of that dependence, one notes that as the affinity decreases (as noted in Table IV by the decrease in a), the value of k_L decreases for the PHE system. A decrease in the affinity of PHE for the column implies an increased overall mass transfer resistance.

The same dependence may be noted for BSA in Table V. The pulse concentration

TABLE V

IMPULSE RESPONSE PARAMETERS ESTIMATES

Run	C_0 *(M)*	*a*	*b (ml/mg)*	k_L *(cm/min)*	Φ_R
1	0.13	5.89	5.346	0.0161	1.208
2	0.13	5.98	2.501	0.0153	0.688
3	0.13	6.94	1.734	0.0167	0.176
4	0.13	8.86	1.375	0.0170	0.170
5	0.13	7.89	0.681	0.0150	0.127
6	0.13	6.35	0.389	0.0135	0.478
7	0.13	5.62	0.330	0.0093	0.642
8	0.13	6.29	0.309	0.0128	0.315
9	0.13	5.64	0.254	0.0098	0.955
10	0.16	1.92	0.719	0.0084	0.220
11	0.16	1.98	0.795	0.0103	0.634
12	0.16	1.93	0.787	0.0113	0.190
13	0.16	2.05	0.361	0.0119	0.508
14	0.16	2.31	0.458	0.0133	0.161
15	0.16	1.95	0.090	0.0134	0.193
16	0.16	1.91	2.604	0.0148	1.333
17	0.16	2.09	1.063	0.0162	0.433
18	0.16	2.31	0.556	0.0178	0.149
19	0.16	1.97	0.175	0.0169	0.169
20	0.16	2.02	0.079	0.0151	0.328
Means ± S.D.:					
	0.13	6.61 ± 1.11		0.0139 ± 0.00285	
	0.16	2.04 ± 0.144		0.0136 ± 0.00292	
Batch equilibrium estimates:					
	0.13	9.54	0.367		
	0.16	2.23	0.0832		

doubles from run 6 to 9; the corresponding k_L value decreases by 32%. A similar change in k_L is noted on comparing runs 6 and 7 (the pulse volume increases from 2.95 to 5.00 ml). Thus, in addition to depending on flow-rate, k_L also depends on factors that affect the local slope of the equilibrium isotherm, such as pH, salt concentration, solute concentration in the pulse and pulse size.

For the lower values of P_P and V_P, estimates of b are much higher than the corresponding batch values. As the pulse volumes and pulse concentrations increase, the value of b approaches the corresponding batch value. The estimate of b shows the strongest dependence on the pulse volume (Fig. 13). Applying the algorithm for determining the required V_P for $0.13N$ and $0.16N$ salt pulses, we obtain values of 3.0 and 3.4 ml, respectively. The estimation technique is conservative as it is based on the calculated peak concentration coming out of the last stage instead of an average over the column. Because of band spreading, this concentration is less than the average peak concentration moving across the column. This safety factor allows for some error in the initial guess of b.

The stage model gives a good fit for the BSA pulse experiments; a representative fit is shown in Fig. 14. The agreement between the isotherm parameters determined by the batch equilibrium method and the impulse response method is good (Fig. 15). For

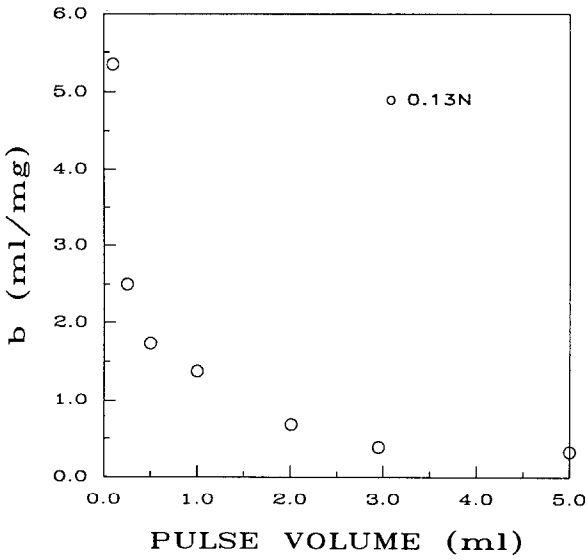

Fig. 13. Dependence of b (ml/mg) on pulse volume (using runs 1–7).

both the batch and pulse experimental estimates of the Langmuir parameters, the exchanger capacity for the protein was in close agreement. This is the ratio a/b, which was estimated to be 26 mg/ml of packed bed. Fig. 15 also illustrates the scatter inherent in batch experiments. The pulse method requires much less manual labor, thus reducing the chances of experimental error and the resulting scatter in data.

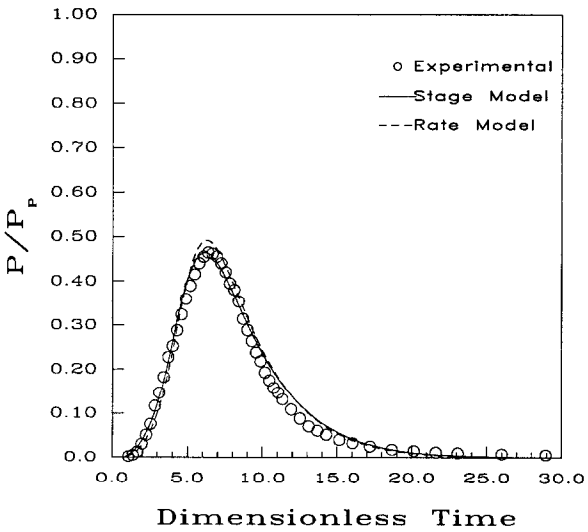

Fig. 14. Typical fit between the response determined from the stage model using the estimated parameter values (BSA–DEAE-Sepharose, run 20) (solid line) and the experimental response (○). A rate model response using the same estimated parameter values is also shown (dashed line).

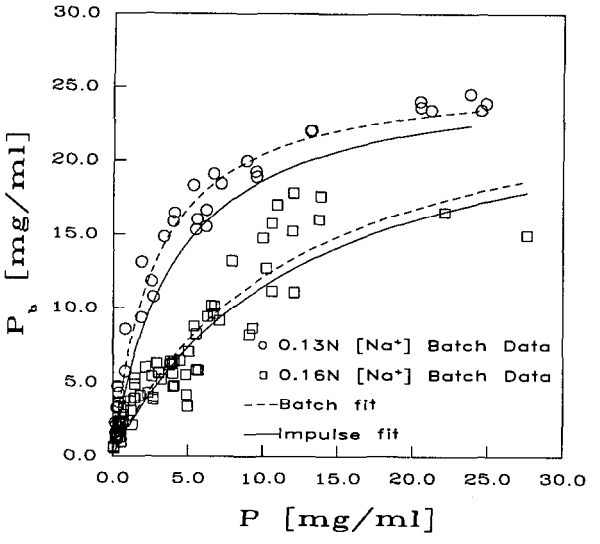

Fig. 15. Typical fit between the equilibrium isotherms determined by the batch equilibrium method (dashed lines) and the impulse response method (solid lines). (○) 0.13 *M* Na^+: $a = 6.61$, $b = 0.254$ ml/mg. (□) 0.16 *M* Na^+: $a = 2.06$, $b = 0.079$ ml/mg.

The economy offered by this technique is significant. The amount of BSA consumed in the batch method was 6.7 g. Following the pulse strategy discussed in this paper, less than 100 mg of BSA (two 5-ml pulses of 10 mg/ml) are required to determine the same isotherms. This 60-fold reduction in the substrate consumption makes this method extremely attractive for determining the isotherm parameters of costly biochemicals. The frontal analysis method lies somewhere in between the batch and pulse methods in terms of solute required; the exact value depends on the equilibrium isotherm. The amount of solute required in both frontal and pulse techniques can be further reduced by using microbore columns.

Comparison with a rate model

Once the equilibrium parameters have been obtained for a system, they may be utilized by more complex models. Fig. 14 shows the rate model discussed in the paper by Yu and Wang[18] in comparison with the stage model in this paper. Both models are using the values of a and b obtained by the stage model. In the ideal case, the rate model could fit the curve more closely as it has more adjustable parameters. However, the mass transfer parameters of the rate model have not been optimized for the curve as that model is not designed for parameter searching. As a result, the stage model fits the data more closely than the rate model.

Parameter searching may require 100 or more runs of a model. As the rate model requires 2 h of CPU time on a Gould NP1 for a single effluent history, parameter searches are conducted by the stage model. The rate model is mainly used to study mass transfer and competition effects in non-linear chromatography. The close agreement between the very different models and the experimental data lends support to the accuracy of parameter estimation by the stage model.

CONCLUSIONS

Rapid and reliable estimates of the Langmuir isotherm parameters can be obtained by the impulse response method. A finite difference Levenberg–Marquardt algorithm proved fast and stable for determining the model parameters. The method is especially useful for determining the non-linear equilibrium isotherms of costly substrates because the substrate consumption is about 2% of that required by the batch equilibrium method. In addition to consuming smaller amounts of costly materials, the pulse method requires less laboratory manipulations. Consequently, the resulting data are less scattered. This method also requires less sorbents for isotherm measurement than the batch method.

The linear driving force for mass transfer is adequate for exchangers with small particle diameters, such as that used in this study. The film mass transfer and pore diffusion effects are approximated by a single mass transfer coefficient. Model simulations show that a small value of the coefficient (representing very slow mass transfer kinetics) results in band splitting of the solute peak. The mass transfer coefficient shows a flow-rate dependence at the lower flow-rates, indicating that film mass transfer is significant under those conditions. The coefficient also depends on particle size, pore concentration (pulse concentration, pulse size and column length) and solute affinity (pH and salt concentration). If extra-column contributions to dispersion are significant, they will appear in the k_L term. These dependences of the lumped parameter approach limit its usefulness in scale-up. This limitation, however, does not appear to affect the accuracy of equilibrium parameter estimation.

The accuracy of the estimation of b depends strongly on the pulse volume and pulse concentration. A strategy to determine the pulse volume and pulse concentration needed for the accurate estimation of b has been developed and used successfully. The equilibrium parameters estimated were applied to a complex rate model and the resulting response compared with the stage model and the experimental data. The stage model represents the pulse experiment as well as the rate model and requires two orders of magnitude less computation time.

ACKNOWLEDGEMENTS

This work was supported by NSF under Grants CBT-8620221 and CEC-88613167. The assistance of F. Liu in collecting some of the data is acknowledged. J. Berninger coded part of the computer program.

SYMBOLS

a	Langmuir isotherm constant
b	Langmuir isotherm constant (ml/mg)
C	counter ion (M)
C_T	total ion concentration in bulk phase (M)
d	column diameter (cm)
$f(P^*)$	equation of the isotherm (mg/ml)
$f'(P^*)$	derivative of $f(P^*)$
K	equilibrium constant, defined by eqn. 2, (ml of bed volume/ml of mobile phase)$^{Z-1}$

k_L overall mass transfer coefficient (cm/min)
L packed height of column (cm)
m number of experimental data points on the response
N number of stages in the column (measure of axial dispersion)
Q mobile phase flow-rate (ml/min)
P substrate ion (mg/ml)
$\hat{P}$ model estimate of substrate ion (mg/ml)
P_b exchanger phase concentration (mg/ml of bed volume)
P_m exchanger capacity (equiv./ml of bed volume)
P_P pulse concentration (mg/ml)
Pe_b axial Peclet number
R radius of the exchanger particles (cm)
SSE sum of squares of error [(mg/ml)^2]
t time coordinate (min)
V volume of each stage (ml)
V^* total pore volume in the column (ml)
V_P volume of the pulse (ml)
Z effective charge on species P
ε_b bed voidage
ε_p exchanger porosity
η defined by eqn. 16
Φ_A defined by eqn. 14a (mg/ml)
Φ_R defined by eqn. 14b
θ dimensionless time
θ_P dimensionless duration of the pulse
$\Delta\theta$ incremental time interval
τ defined by eqn. 7b (min)

Subscripts
b bound state
j jth stage
k kth time interval
0 initial value
P pulse
T total

REFERENCES

1 W. Kopaciewicz, M. A. Rounds, J. Fausnaugh and F. E. Regnier, *J. Chromatogr.*, 266 (1983) 3.
2 T. K. Sherwood, R. L. Pigford and C. R. Wilke, *Mass Transfer*, McGraw-Hill, New York, 1975.
3 G. Scatchard, I. H. Scheinberg and S. H. Armstrong, Jr., *J. Am. Chem. Soc.*, 72 (1950) 535.
4 T. W. Hutchens, T.-T. Yip and J. Porath, *Anal. Biochem.*, 170 (1988) 168.
5 R. D. Whitley, R. Wachter, F. Liu and N.-H. L. Wang, *J. Chromatogr.*, 465 (1989) 137.
6 J. F. K. Huber, in M. Van Swaay (Editor), *Gas Chromatography*, Butterworths, London, 1962, p. 26.
7 J. F. K. Huber and R. G. Gerritse, *J. Chromatogr.*, 58 (1971) 137.
8 J. Jacobson, J. Frenz and Cs. Horváth, *J. Chromatogr.*, 316 (1984) 53.
9 J.-X. Huang and Cs. Horváth, *J. Chromatogr.*, 406 (1987) 275.
10 J.-X. Huang and Cs. Horváth, *J. Chromatogr.*, 406 (1987) 285.
11 D. B. Shah and D. M. Ruthven, *AIChE J.*, 23 (1977) 804.

12 P. Schneider and J. M. Smith, *AIChE J.*, 14 (1968) 886.
13 N. Wakao, S. Kaguei and J. M. Smith, *Ind. Eng. Chem., Fundam.*, 19 (1980) 363.
14 F. H. Arnold, H. W. Blanch and C. R. Wilke, *Chem. Eng. J.*, 30 (1985) B25.
15 S. H. Hyun and R. P. Danner, *Ind. Eng. Chem., Fundam.*, 24 (1985) 95.
16 N. F. Kirkby, N. K. H. Slater, K. H. Weisenberger, F. Addo-Yobo and D. Doulia, *Chem. Eng. Sci.*, 41 (1986) 2005.
17 J. L. Wade, A. F. Bergold and P. W. Carr. *Anal. Chem.*, 59 (1987) 1286.
18 Q. Yu and N.-H. L. Wang, *Comput. Chem. Eng.*, 13 (1989) 915.
19 A. Velayudhan and Cs. Horváth, *J. Chromatogr.*, 443 (1988) 13.
20 P. L. Cen and R. T. Yang, *AIChE J.*, 32 (1986) 1635.
21 L. R. Petzold, *DASSL: A Differential/Algebraic System Solver*, Sandia National Laboratories, Livermore, CA, 1982.
22 T. Dogu, *AIChE J.*, 32 (1986) 849.
23 H. C. Thomas, *J. Am. Chem. Soc.*, 66 (1944) 1664.
24 N.-H. L. Wang, Q. Yu and S. U. Kim, *React. Polym.*, in press.
25 J. M. Brown, *M. S. Thesis*, Purdue University, 1989.
26 P. C. Wankat, *Large-Scale Adsorption and Chromatography, Volume I: Chromatographic Analysis*, CRC Press, Boca Raton, FL, 1986.
27 C. DeLisi, H. W. Hethcote and J. W. Brettler, *J. Chromatogr.*, 240 (1982) 283.
28 A. L. Myers and S. Byington, in A. E. Rodrigues (Editor), *Ion Exchange Science and Technology* (*NATO ASI Series, Series E*, No. 107), Martinus Nijhoff, Dordrecht, 1986.